International Journal of Solids and Structures 000 (2017) 1–11

Contents lists available at ScienceDirect

International Journal of Solids and Structures

journal homepage: www.elsevier.com/locate/ijsolstr

Modeling of kinematic hardening at large biaxial deformations in pearlitic rail steel

Knut Andreas Meyer[a,*], Magnus Ekh[a], Johan Ahlström[b]

[a] Division of Material and Computational Mechanics, Department of Industrial and Materials Science, Chalmers University of Technology, Gothenburg, 412 96, Sweden
[b] Division of Engineering Materials, Department of Industrial and Materials Science, Chalmers University of Technology, Gothenburg, 412 96, Sweden

ARTICLE INFO

Article history:
Received 7 June 2017
Revised 30 August 2017
Available online xxx

Keywords:
Axial-Torsion
Pearlitic steel
Biaxial
Multiaxial
Finite strains

ABSTRACT

Using an Axial-Torsion testing machine, pearlitic R260 steel specimens are twisted until fracture under different axial loads. A well established framework for finite elastoplasticity with kinematic hardening is used to model the deformation of the specimens. In particular, we evaluate the ability of different kinematic hardening laws to predict the observed biaxial load versus displacement response. It is found that the combination of Armstrong–Frederick dynamic recovery and Burlet–Cailletaud radial evanescence saturation is efficient even for the large strains achieved in this study. The results are less conclusive on the appropriateness of replacing the Armstrong–Frederick with an Ohno–Wang type of kinematic hardening law.

1. Introduction

Large shear strains accumulate close to the running band of railway rails and wheels during service (see e.g. Alwahdi et al., 2013; Cvetkovski and Ahlström, 2013). The connection to crack initiation is well established, see Johnson (1989) for an overview. Additionally, plastic flow and wear cause changes in the geometry, altering the contact loading conditions. Hence, accurate constitutive models for cyclic large strain plasticity are important components for the prediction of the fatigue life of wheels and rails. This work considers experiments and modeling of cyclic large strain plasticity of one of the most common rail steels, the pearlitic grade R260.

The load on the rail consists of a large hydrostatic compressive stress due to the normal contact, and shear stresses mainly due to traction and cornering. Severe plastic deformation techniques, such as Plane Stress Local Torsion (PSLT), High Pressure Torsion (HPT) and Equal Channel Angular Pressing (ECAP), have been applied by several authors (e.g. Hohenwarter et al., 2011; Ivanisenko et al., 2002; Khoddam et al., 2014; Wetscher et al., 2007) to mimic these loading conditions. Significant strain localization occurs in PSLT testing which makes further characterization difficult. HPT testing has been particularly successful in obtaining a severely deformed microstructure under controlled laboratory conditions. While able to replicate the strains, the two latter processes are difficult to use for direct model evaluations due to the complex contact conditions. Several authors (e.g. Estrin et al., 2008; Wei et al., 2014; Larijani et al., 2015; Yoon et al., 2008; Kim, 2001; Draï and Aour, 2013) have simulated the HPT process, and Larijani et al. (2015) even simulated the extraction of specimens from the deformed disks and their uniaxial response. However, multiaxial loading of the extracted specimens is challenging, due to the limited size that can be extracted with a reasonable homogeneous deformation.

The first objective of this paper is to investigate the possibility of using an Axial-Torsion testing machine to obtain large shear strains in cylindrical test specimens. Such predeformed specimens can in future works be used in Low Cycle Fatigue (LCF) experiments, determining the influence of large strains on the multiaxial LCF behavior. This avoids the complicated contact conditions present in ECAP and HPT testing, and enables evaluation of the material response during large deformations. To investigate the potential to reach high shear strains, the amount of twisting that the specimens can endure before failure is evaluated for different axial loads.

The second objective of this paper is to identify appropriate cyclic plasticity models for modeling the large biaxial strains from the experiments. Many constitutive models for cyclic metal plasticity, such as the Chaboche model (Chaboche, 1986) and Ohno–Wang (Ohno and Wang, 1993a), are known to over-predict multiaxial ratcheting (e.g. Abdel-Karim, 2009; Bari and Hassan, 2002; Portier et al., 2000; Chen et al., 2005). Delobelle et al. (1995) suggested to use a linear combination of the Armstrong–Frederick dynamic recovery term and the radial evanescence term introduced by Burlet and Cailletaud (1986). This suggestion was

* Corresponding author.
E-mail address: knut.andreas.meyer@chalmers.se (K.A. Meyer).

https://doi.org/10.1016/j.ijsolstr.2017.10.007
0020-7683/

Table 1
% mass composition of the R260 steel, analyzed according to ASTM E 572, 1086 and 1029.

C	Si	Mn	P	S	Cr	Al	V	N	Cu
0.72	0.31	1.04	0.006	0.01	0.02	< 0.002	< 0.005	0.006	0.018

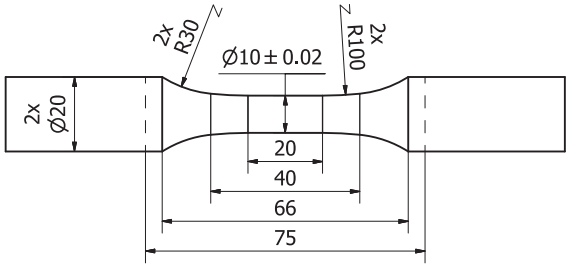

Fig. 1. Specimen dimensions in mm. Dashed lines indicate grip positions.

shown to solve some issues in modeling multiaxial ratcheting. Johansson et al. (2005a) formulated the combined Armstrong–Frederick and Burlet–Cailletaud rule using the hyperelasto-plastic framework from Wallin et al. (2003). Promising results were obtained in Johansson et al. (2005a) when this model was compared to the small strain test data from Hassan et al. (1992). These findings have not, however, been confirmed for large inelastic deformations. This is evaluated in the present study, where we investigate how well different kinematic evolution laws are able to predict the response for large shear strains.

It is commonly known that the yield surface distorts during plastic deformations (see e.g. Sung et al., 2011, and references therein). Several modeling approaches have proved successful at modeling this distortional hardening (e.g. Barthel et al., 2008; Harrysson et al., 2007; Pietryga et al., 2012), and much work has been conducted on the theoretical derivations of such models (e.g. Feigenbaum and Dafalias, 2007; Harrysson et al., 2007; Menzel and Steinmann, 2003; Plesek et al., 2010; Shi et al., 2014). However, the experiments in the present work cannot clearly differentiate between different yield surface evolutions. We therefore limit this study to investigate whether a kinematic hardening law with an isotropic yield surface can describe the mechanical response. The evaluation of the yield surface distortion is left for future work.

This paper is organized as follows:

- In Section 2 the experimental setup and results are presented.
- In Section 3 the modeling framework and the different kinematic evolution laws are described.
- In Section 4 the methodology for obtaining the set of material parameters that best fit the experimental data is presented.
- In Section 5 the ability of the different models to fit and predict the experimental results is evaluated. We also compare the residual shear stresses for different models.

2. Experiments

Test bars were extracted about 20 mm below the surface of new pearlitic R260 rails heads, with the material composition given in Table 1. The bars were turned between centers to the dimensions given in Fig. 1. A smooth transition with radius of 100 mm was used to minimize the strain concentration at the end of the gauge section. The tests were conducted on an Axial-Torsion MTS test rig, with load cell capacities of 100 kN and 1100 Nm, and a torsional stroke of 90 deg. To deform the specimens, the following load sequence was used

1. Ramp axial load
2. Rotate 90 deg in 60 s, maintaining the axial load
3. Relax the axial and the torsional load
4. Open lower grip, rotate back and close grip. Go to 1.

Failure was detected when the torque dropped 2 Nm below the maximum value during the current load cycle. No false failures were detected using this criterion, but some specimens with tensile axial load fractured completely at failure detection.

An MTS 632.80 extensometer with a 12 mm gauge length was used to obtain the initial Young's modulus E and shear modulus G accurately. As the extensometer range was limited to ±6 deg/12 mm, the machine piston positioning sensors were used to measure specimen deformations. To reduce the influence from the machine deformations, the stiffness of the machine was quantified and compensated for (See Appendix A for further details). To ensure consistent results, the grips were positioned 75 mm apart at the beginning of each experiment.

Table 2
Elastic material parameters and initial yielding.

Parameter	Value	Std. dev.	Unit	N_{tests}
E	212.0	0.5	GPa	9
G	80.5	0.5	GPa	3
$R_{p0.01}$	388.5	5.4	MPa	9
$R_{p0.05}$	466.6	6.2	MPa	9
$R_{p0.2}$	534.2	6.8	MPa	2

2.1. Elastic material parameters

The initial elastic material parameters were calibrated using the extensometer data from the first load cycle. For Young's modulus, nine specimens were available using the initial ramp of the axial load. This data was also used to obtain the yield limits. Only the three tests with zero axial load were used to calculate the shear modulus. The values of the elastic parameters and the yield limits are presented in Table 2. It should be noted that while the elastic parameters are rather certain, the yield limits show larger spread. This is expected as the yielding is not distinct, which is also reflected in the difference between the yield definitions.

2.2. Experimental results

The results in terms of specimen length changes and torque responses for different axial loads are shown in Fig. 2. There is a strong influence of the axial loading on the torque response, which is mainly due to the nonlinear geometrical effect. For a nominal axial stress $\bar{P}_a = -500$ MPa the specimen diameter increases uniformly by approximately 12%, and the overall length decreases by about 7.5 mm. The initial torque is highest for zero axial load, followed by $\bar{P}_a = \pm 250$ MPa, see Fig. 2b. The torque increases faster for the compressive axial loads as the diameter starts to increase. For tensile axial loads, the diameter decreases uniformly and the torque quickly saturates. The behavior described above is mainly a result of material hardening and geometric changes.

From Fig. 2 it is clear that the amount of twist a specimen can withstand before failure is increasing significantly with the axial compressive stress. The amount of surface shear strain increases even more, due to the shortening of the specimen and the increase of gauge diameter. Higher compressive stresses than 600 MPa were not used in order to avoid buckling during twisting.

Please cite this article as: K.A. Meyer et al., Modeling of kinematic hardening at large biaxial deformations in pearlitic rail steel, International Journal of Solids and Structures (2017), https://doi.org/10.1016/j.ijsolstr.2017.10.007